

Demonstration of an optoelectronic interconnect architecture for a parallel modified signed-digit adder and subtracter

De-Gui Sun, MEMBER SPIE
University of Texas at Austin
Microelectronics Research Center
Department of Electrical and Computer
Engineering
Austin, Texas 78712

Na-Xin Wang
Wuxi Institute of Light Industrial Technology
Department of Mechanics
Wuxi, Jiangsu 214036, China

Liming He
Jilin Institute of Technology
Department of Electrical Engineering
Changchun, Jilin 130025, China

Zhao-Heng Weng, MEMBER SPIE
Daheng Wang, MEMBER SPIE
Academic Sinica
Changchun Institute of Optics and Fine
Mechanics
Changchun, Jilin 130022, China

Ray T. Chen, MEMBER SPIE
University of Texas at Austin
Microelectronics Research Center
Department of Electrical and Computer
Engineering
Austin, Texas 78712
E-mail: raychen@uts.cc.utexas.edu

1 Introduction

There are two options for developing parallel digital optical computing systems: one is to research the carry-free or carry-limited parallel algorithm, the other is to research the optical implementing architecture. Of course, the best selection is an effective combination of these two options. The modified signed-digit (MSD) algorithm is an effective carry-free or carry-limited algorithm, and symbolic substitution is an optical parallel implementing approach. Thus, an optical MSD parallel computing system based on symbolic substitution is a typical example of a combination of a parallel algorithm and a parallel implementation approach.¹⁻⁵ Especially in recent years, new MSD architectures have been proposed and studied.⁶⁻¹² In fact, the important factor for the realization of the conversion from the algorithm to the hardware structure is having an effective encoding scheme, so the research on encoding schemes has received more attention as an important content in digital optical computing.⁹⁻¹⁷ At the same time, improved encoding methods have been proposed and studied.^{10-12,15-17} These improved encoding schemes, especially space-variant encoding, not only expand encoding theory but also

Abstract. A space-position-logic-encoding scheme is proposed and demonstrated. This encoding scheme not only makes the best use of the convenience of binary logic operation, but is also suitable for the trinary property of modified signed-digit (MSD) numbers. Based on the space-position-logic-encoding scheme, a fully parallel modified signed-digit adder and subtracter is built using optoelectronic switch technologies in conjunction with fiber-multistage 3-D optoelectronic interconnects. Thus an effective combination of a parallel algorithm and a parallel architecture is implemented. In addition, the performance of the optoelectronic switches used in this system is experimentally studied and verified. Both the 3-bit experimental model and the experimental results of a parallel addition and a parallel subtraction are provided and discussed. Finally, the speed ratio between the MSD adder and binary adders is discussed and the advantage of the MSD in operating speed is demonstrated. © 1996 Society of Photo-Optical Instrumentation Engineers.

Subject terms: parallel algorithm; parallel architecture; space-position-logic-encoding; optoelectronic switch and interconnect technologies; modified-signed-digit adder and subtractor.

Paper 20045 received Apr. 14, 1995; revised manuscript received Nov. 13, 1995; accepted for publication Nov. 14, 1995.

make best use of the parallelisms of both optics and the MSD algorithm, thus playing an important role in parallel digital optical computing. However, in the proposed space encodings, because some patterns are required to represent operand bits, the space size taken by each operand bit cannot be made very small, which limits the miniaturization and integration of MSD optical computing systems. Multilayer and multistage optical interconnection is another important parallel implementation approach in digital optical computing that can help the switches to complete logic operations as well as implement data transportation and switching.

Optoelectronic interconnects have shown a promising future as the hardware approach of digital optical computing because they can be compatible with microstructure optoelectronic switch technologies.^{12,18-21} In addition, multilayer and multistage optoelectronic interconnects, as the hardware approach of parallel digital optical computing, are suitable for controlling the digitized signal connections and operations as well as for exploiting some optical advantages such as higher bandwidth and lower crosstalk. In digital optical computing, perfect shuffle, crossover, and butterfly are three typical interconnect networks,²²⁻²⁴

	T_{i+1}		
X_i			
1	1	1	0
0	1	0	$\bar{1}$
$\bar{1}$	0	$\bar{1}$	$\bar{1}$
Y_i	1	0	$\bar{1}$

	W_i		
X_i			
1	0	$\bar{1}$	0
0	$\bar{1}$	0	1
$\bar{1}$	0	1	0
Y_i	1	0	$\bar{1}$

(a)
(b)

Fig. 1 Truth tables of the first-step operation of MSD addition: (a) for transfer digits T_{i+1} and (b) for weight digits W_i .

among which the butterfly has been proved to have some advantages over the others in optical computing.^{25,26} Addition and subtraction are the most primitive arithmetic operations in digital computation. Almost all of the other arithmetic operations such as multiplication, division, and some special functions must be performed based on addition and subtraction. The purpose of this paper is to present the implementation of a fully parallel MSD adder and subtracter based on the effective combination of the MSD algorithm and the butterfly interconnection architecture by use of a space-position-logic-encoding (SPLE) scheme that exploits both the carry-free property of the MSD algorithm and the convenience of binary logic operation with optoelectronic logic technology. A 3-bit experimental model of a parallel adder and subtracter based on the MSD algorithm and fiber interconnect technology is built, and correct experimental results are provided. To interface the parallel optoelectronic adder architecture with the conventional electronic computers in the near future, the conversion and brief comparison between the MSD and binary additions are carried out, and the advantage of our MSD adder in speed is demonstrated.

2 MSD Algorithm Review

An MSD bit can be written as

$$D_{MSD} = [1, 0, \bar{1}], \tag{1}$$

where $\bar{1}$ represents -1 . Each MSD bit has three values for selection (i.e., 1, 0, and -1). These three possible values 1, 0, and $\bar{1}$ of each MSD bit are called digits. Then each decimal number can be represented in the MSD number system by the coefficients of the polynomial¹⁻³:

$$D_{10} = [1, 0, \bar{1}]2^{n-1} + \dots + [1, 0, \bar{1}]2^i + \dots + [1, 0, \bar{1}]2^0. \tag{2}$$

For example, a decimal number 27 would be written as:

$$(27)_D = 1 \cdot 2^4 + 1 \cdot 2^3 + 0 \cdot 2^2 + 1 \cdot 2^1 + 1 \cdot 2^0 = [11011]_{MSD}.$$

$$(27)_D = 1 \cdot 2^4 + 1 \cdot 2^3 + 1 \cdot 2^2 + (-1) \cdot 2^1 + 1 \cdot 2^0 = [111\bar{1}1]_{MSD}.$$

$$(27)_D = 1 \cdot 2^4 + 1 \cdot 2^3 + 1 \cdot 2^2 + 0 \cdot 2^1 + (-1) \cdot 2^0 = [1110\bar{1}]_{MSD}.$$

Note that the first selection $[11011]_{MSD}$ is the same as a binary number, so it can be said that the binary number is only a special form of the MSD number. This feature is a basis for the conversion from an MSD number to a binary one, as discussed in Sec. 6.

For two MSD numbers, $X_{MSD}[X_{n-1}, \dots, X_i, \dots, X_0]$ and $Y_{MSD}[Y_{n-1}, \dots, Y_i, \dots, Y_0]$, the addition can be performed through a three-step operation.¹⁻³ At the first step, a weight digit W_i and a transfer digit T_{i+1} , which are MSD bits, are produced by

$$X_i + Y_i = 2T_{i+1} + W_i, \tag{3}$$

where all the values of T_{i+1} and W_i are only related to X_i and Y_i , and determined by their truth tables, as shown as Figs. 1(a) and 1(b), respectively.

At the second step, another pair of weight digit W'_i and transfer digit T'_{i+1} is produced by

$$W_i + T_i = 2T'_{i+1} + W'_i, \tag{4}$$

where all the values of T'_{i+1} and W'_i are related only to W_i and T_i and are determined by their truth tables, as shown in Figs. 2(a) and 2(b), respectively.

The third step generates the final sum digit S_i :

$$S_i = W'_i + T'_i, \tag{5}$$

where all the values of S_i are related only to W'_i and T'_i and are given by the truth table, as shown in Fig. 3, which is the same as Fig. 1(a). In the same step of operations, all the operations among the different bits are the same, thus Figs. 1, 2, and 3 all indicate only the 1-bit operations. In terms of the three-step operations of MSD addition, the MSD addition of two 3-bit numbers can be depicted in the butterfly interconnection architecture as shown in Fig. 4, where $X (= X_2X_1X_0)$ and $Y (= Y_2Y_1Y_0)$ are augend and addend, respectively, and $Z (= Z_3Z_2Z_1Z_0)$ is the final addition result.

3 Space-Position-Logic-Encoding Scheme

As described, the difference between the MSD bit and the binary bit is that the binary bit has only two selections, 1 and 0, while the MSD bit has three selections, 1, 0, and $\bar{1}$, respectively. Therefore, it is unlike the binary bit, which uses higher and lower voltages as an encoding scheme. In digital optical computing, because of optical properties and the symbolic substitution theorem, pattern encoding, polarization encoding^{2-8,12-14} and other encoding schemes^{9-11,15-17} occur successively. According to the characteristics of the MSD numbers and the optical properties, we propose an SPLE scheme, as shown in Fig. 5(a), in which three different space positions, A, B, and C (or a, b, and c), are used to represent 1, 0, and $\bar{1}$ of MSD bits in which three light-emitting diodes (LEDs) or laser diodes (LDs) at A, B, and C (or a, b, and c) represent only one MSD bit; namely, only one LED or LD has a light signal, and a light signal at a different position of the i 'th bit

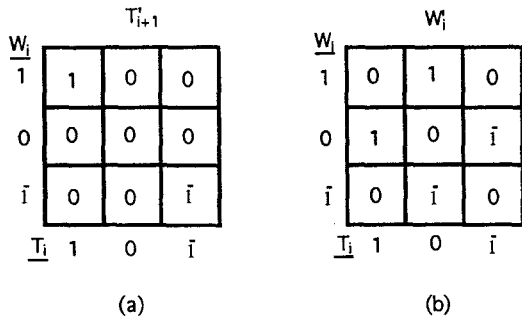


Fig. 2 Truth tables of the second-step operation of MSD addition: (a) for transfer digits T_{i+1} (b) for weight digits W_i .

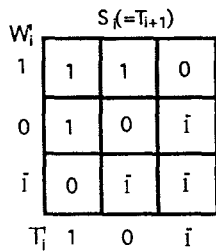


Fig. 3 Truth table of the third step of 3-bit MSD addition and subtraction for the final sum S_i .

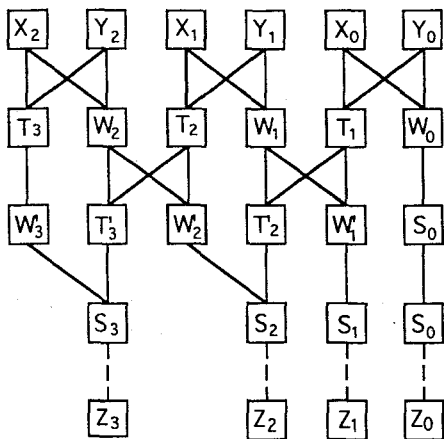


Fig. 4 Butterfly architecture implementing operation of MSD addition.

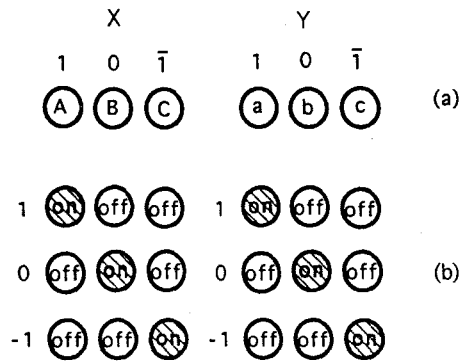


Fig. 5 SPLE scheme: (a) three space position codes, A, B, and C (or a, b, and c), stand for 1, 0, and $\bar{1}$, respectively, and (b) three work states of A, B, and C (or a, b, and c).

represents a different value. The combination of all their work states is shown in Fig. 5(b). For example, the light signal of the LED or the LD at position A of the X_i bit represents $X_i=1$, and at the same time, the LEDs or LDs at positions B and C of the X_i bit have no light signals. Thus each space position has two states, either having a light signal or having no light signal, which is similar to the logic operations of the binary algorithm. Therefore it is an SPLE scheme. Then with the SPLE scheme, the truth tables for the three operations of MSD additions, as shown in Figs. 1, 2, and 3, become the new forms, as shown in Figs. 6, 7, and 8, where any table has nine states [i.e., the nine combinations of the three digits (A, B, and C) of augend X_i and the three digits (a, b, and c) of addend Y_i]. The three digits of the augend are arranged in a column and the three digits of the addend are arranged in a row, as shown in Figs. 6, 7, and 8. Of course, each state is an AND result of two digits.

4 Butterfly Interconnect Architecture

In terms of all the truth tables of MSD addition expressed in the SPLE scheme, any table has nine states, and each state is an AND result of two digits from a row and a column, respectively. Thus we can use a unitary detecting array including nine detecting elements to stand for all the truth tables of MSD addition, as shown in Fig. 9, in which

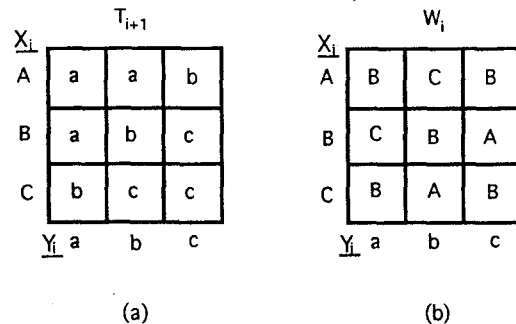


Fig. 6 Truth tables of the first-step operation of MSD addition represented by the SPLE scheme: (a) for transfer digits T_{i+1} and (b) for weight digits W_i .

		T'_{i+1}		
W_i				
A	a	b	b	
B	b	b	b	
C	b	b	c	
	T_i	a	b	c

		W_i		
W_i				
A	B	A	B	
B	A	B	C	
C	B	C	B	
	T_i	a	b	c

Fig. 7 Truth tables of the second-step operation of MSD addition represented by the SPLE scheme: (a) for transfer digits T'_{i+1} and (b) for weight digits W_i .

all the detecting elements (G_1, \dots, G_9) can be used for the nine states of any truth table. Note that G_1 is the detecting element for the AND operation of A and a, G_2 is the detecting element for the AND operation of A and b, and so forth, until G_9 is the detecting element for the AND operation of C and c. To build a multilayer butterfly interconnection architecture corresponding to the multibit computing, for every step operation of any bit computation, we use the most basic butterfly to represent the nine AND operations (Fig. 9) of three augend digits (A, B, and C) and three addend digits (a, b, and c) as shown in Fig. 10. It can be noted with ease that the nine combinations come from 11 pairwise combinations of 12 operand bits (double A, B, C and a, b, c). This butterfly interconnect architecture is the easiest because all the interconnection operations are performed between two adjacent nodes, and it is especially suitable for microstructures such as gratings and waveguides. No matter how many bits of MSD addition and subtraction. There are only four switch modules in conjunction with three stages of multilayer butterfly interconnects, as shown in Fig. 10. For example, an N -bit MSD adder and subtracter requires each switch module to have N rows of switch cells corresponding to N -layer interconnects.

The AND results from the nine detecting elements on the detecting planes of switch modules can drive several LEDs or LDs on the light-emitting planes, which give light signals for the next operations. The arrangement of all the possible light signals (A, B, and C; a, b, and c) on the light-emitting planes of modules is the same as that in Fig.

		$S_i (=T'_{i+1})$		
W_i				
A	a	a	b	
B	a	b	c	
C	b	c	c	
	T_i	a	b	c

Fig. 8 Truth table of the third-step operation MSD addition represented by SPLE scheme for the final sum S_i .

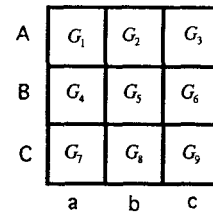


Fig. 9 Unitary detecting array, where G_1, G_2, \dots, G_9 are nine detecting elements.

10, but only the detecting elements receiving two light signals can perform AND operations and make their LEDs or LDs produce light signals at the corresponding positions. Figures 11(a), 11(b), and 11(c) represent the operating examples of $X_i=1$ and $Y_i=1$, $W_i=1$ and $T_i=0$, and $W'_i=0$ and $T'_i=0$, respectively. Obviously each MSD bit addition is completed through three stages of the simplest butterfly interconnections and three operations, as shown in Fig. 11, where hatched circles indicate having light signals, and hollow circles indicate having no light signals. For the first stage of operations, as shown in Fig. 11(a), if $X_i=1$ and $Y_i=1$ (i.e., A_i and a_i have light signals), then only the detecting element G_1 can receive two light signals and perform AND operations and can drive its next-stage LEDs or LDs a of T'_{i+1} and B of W_i for the next stage of operations according to Figs. 6(a) and 6(b), respectively. For the second stage of operations, as shown in Fig. 11(b), if $W_i=1$ and $T_i=0$ (i.e., A_i and b_i have light signals), then only the detecting element G_2 can receive two light signals and perform AND operations and can drive its next-stage LEDs or LDs b of T'_{i+1} and A of W'_i for the next stage of operations according to Figs. 7(a) and 7(b), respectively. For the third stage of operations, as shown in Fig. 11(c), if $W'_i=0$ and $T'_i=0$ (i.e., B_i and b_i have light signals), then only the detecting element G_5 can receive two light signals and perform AND operations and can drive its next-stage LEDs or LDs b of S_i of the i 'th bit according to Fig. 8. The interconnections among all the operand bits can be performed according to the standard butterfly structure as shown in Fig. 4, which can be implemented by use of electrical interconnection or optical guided-wave interconnection within the switch modules. The interconnections among the 12 positions of two groups of operand digits can be completed by use of optical interconnections such as gratings and fibers. Therefore with the SPLE scheme and the simplest butterfly interconnections, a fully parallel MSD adder can be constructed by use of three stages of optical butterfly

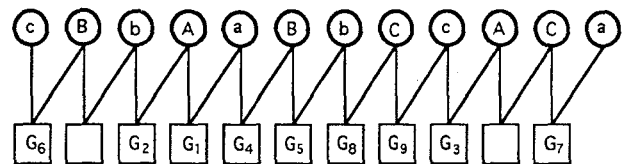


Fig. 10 Corresponding architecture of operands (A, B, and C; a, b, and c) represented by the simplest butterfly interconnection.

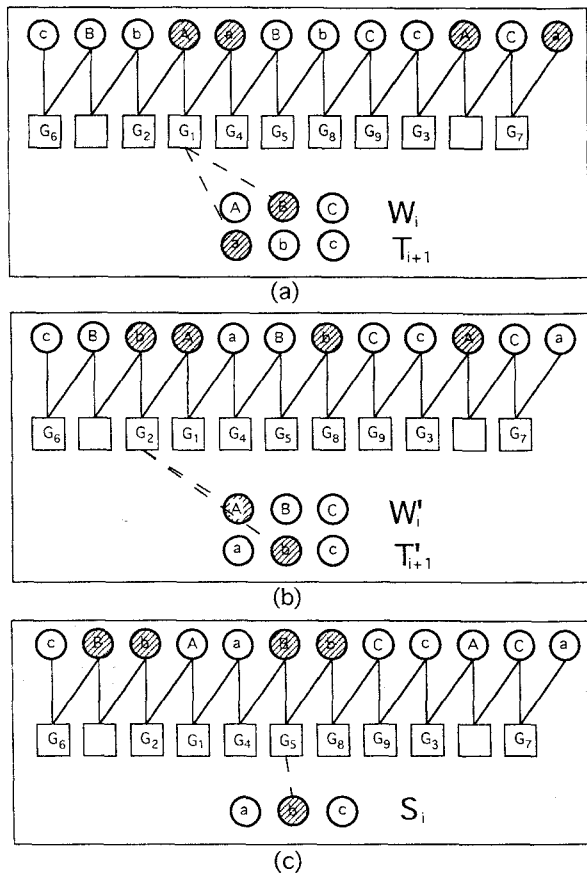


Fig. 11 Operation examples of an MSD adder and subtracter: (a) $X_i=1$ and $Y_i=1$; (b) $W'_i=1$ and $T'_i=0$; and (c) $W'_i=0$ and $T'_i=0$. Hatched circles indicate having light signals, and hollow circles indicate having no light signals.

interconnection and four switch modules, M_0 , M_1 , M_2 , and M_3 , which can complete logic operations and signal arrangements, as shown in Fig. 12, where Fig. 12(a) is the schematic construction of a 3-bit optoelectronic MSD adder, and Fig. 12(b) is the circuit of each switch cell of optoelectronic switch modules. The circuit is constituted by using photosensitive diodes, LEDs, bipolar transistors, and their associated electronic devices to implement the AND operations. Because all the switch cells are required to perform AND operations of two adjacent nodes, the whole switch module has many of the same circuits as shown in Fig. 12 and can reliably work. This can be verified by the experimental results of the logic performance of this optoelectronic switch as shown in Fig. 13, where Fig. 13(a) is the state of one-signal forcing, and Fig. 13(b) is the state of two-signal forcing. Because the two input signals are the same, only one input signal curve is shown in both Figs. 13(a) and 13(b). In either figure, the upper curve is the input signal, and the lower curve is the AND operation result of two input signals. With the SPLE scheme, the MSD subtraction can also be performed as MSD addition by use of the complement of the subtrahend (i.e., with 1 as $\bar{1}$, $\bar{1}$ as 1, and 0 as 0 in the subtrahend). Therefore, the MSD architecture in this paper is really a 3-bit parallel optoelectronic MSD adder and subtracter.

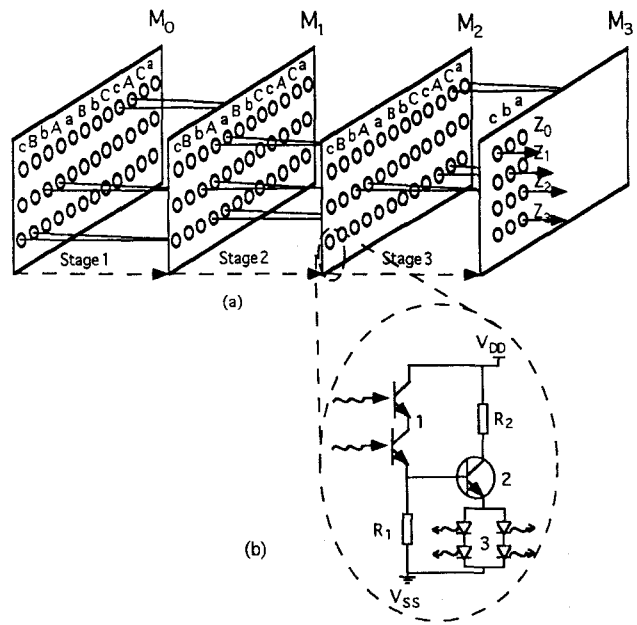


Fig. 12 Architecture of an optoelectronic MSD adder and subtracter—four switch modules and three stages of the simplest butterfly interconnection: (a) construction and (b) the circuit of a switch cell, where 1, photo-diode; 2, bipolar transistor; and 3, LEDs.

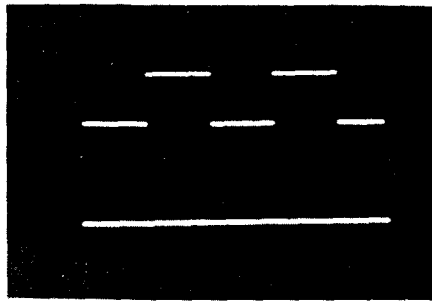
5 Experiments

With optoelectronic and fiber interconnect technologies, an experimental model of 3-bit optoelectronic parallel MSD adder and subtracter was built by us, as shown in Fig. 14, and the correct experimental results were obtained.

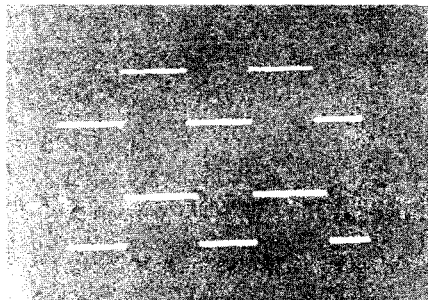
For example, the addition of 6 and 5, $(6)_{10} + (5)_{10} = (11)_{10}$, is the addition of two 3-bit MSD numbers. As described in Sec. 2, one decimal number can have several MSD forms for selection. For convenience, we just select the form which is the same as binary representation, so the addition of 6 and 5 can also be written as $(110)_{MSD} + (101)_{MSD}$. The signal pattern and experimental result of the input signals are shown as in Figs. 15(a) and 15(b), respectively, and both the simulation and experimental results of their addition are obtained, as shown in Figs. 16(a) and 16(b), respectively, where filled circles indicate having light signals and hollow circles indicate having no light signals. It can be noted from Figs. 16(a) and 16(b) that both simulation and experimental results are $(1101)_{MSD} = (11)_{10}$, which are obviously correct. For the subtraction of 7 and 7, $(7)_{10} - (7)_{10} = (0)_{10}$ can also be written as $(111)_{MSD} + (\bar{1}\bar{1}\bar{1})_{MSD}$; the signal pattern and experimental result of input signals are shown as Figs. 17(a) and 17(b), respectively, and both the simulation and experimental results of their subtraction are obtained as shown in Figs. 18(a) and 18(b), respectively, where filled circles indicate having light signals and hollow circles indicate having no light signals. It can be noted from Figs. 18(a) and 18(b) that both simulation and experimental results are $(0000)_{MSD} = (0)_{10}$, which are obviously correct.

6 Conversion Between the MSD Adder and Binary Ones

We know from the preceding demonstrations that results of these MSD additions are generally MSD digits. Thus it is



(a)



(b)

Fig. 13 Experimental results of logic performance of an optoelectronic switch module; (a) the state of one-signal forcing and (b) the state of two-signal forcing, where the upper curve is the input signal, and the lower curve is the AND operation result.

necessary to convert the MSD digits into binary ones to interface this parallel MSD adder with current electronic computers. At the same time, we can also compare the MSD adder with binary ones in operating speed. In fact, this work has been started by Hwang and Louri.³

We assume an output result from the MSD adder is Z_m . To convert it into the binary form Z_b , we can separate Z_m into two parts Z_m^+ and Z_m^- . Because the Z_b comes from the

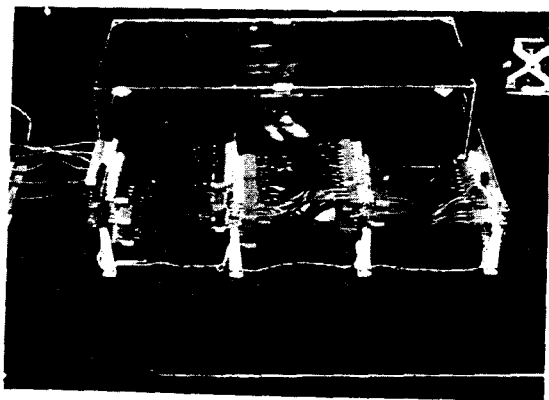
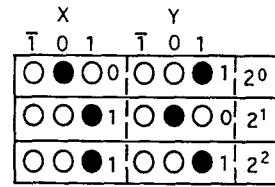


Fig. 14 Experimental model of 3-bit MSD adder and subtracter by use of optoelectronic logic and fiber interconnection technologies.

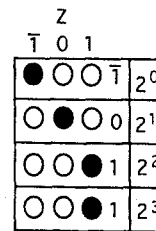


(a)



(b)

Fig. 15 Signal pattern and experimental result of an MSD addition— $(6)_{10} + (5)_{10} = (110)_{MSD} + (101)_{MSD}$: (a) signal pattern and (b) experimental result.

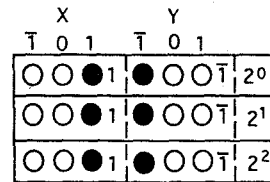


(a)

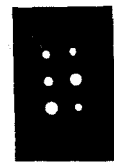


(b)

Fig. 16 Simulation and experimental results of an MSD addition— $(6)_{10} + (5)_{10} = (110)_{MSD} + (101)_{MSD}$: (a) simulation result and (b) experimental result.

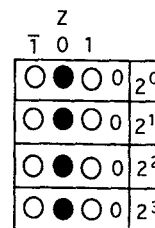


(a)

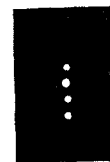


(b)

Fig. 17 Signal pattern and experimental result of an MSD subtraction— $(7)_{10} - (7)_{10} = (111)_{MSD} + (\bar{1}\bar{1}\bar{1})_{MSD}$: (a) signal pattern and (b) experimental result.



(a)



(b)

Fig. 18 Simulation and experimental results of an MSD subtraction— $(7)_{10} - (7)_{10} = (111)_{MSD} + (\bar{1}\bar{1}\bar{1})_{MSD}$: (a) simulation result and (b) experimental result.

original Z_m , their values should be equal to each other, but their representations are different, so the MSD addition can be depicted in Eq. (6):

$$Z_b = Z_m = Z_m^+ + Z_m^- \quad (6)$$

where Z_m^+ can be obtained by replacing $\bar{1}$ with 0 and keeping all the 0 and 1 unchanged in Z_m , while Z_m^- can be obtained by replacing 1 with 0 and keeping all the 0 and $\bar{1}$ unchanged in Z_m . For a positive Z_m , its most significant bit $Z_m(n)$ must be 1, so the most significant bit of Z_m^+ , $Z_m^+(n)$, must be 1 also, while the most significant bit of Z_m^- , $Z_m^-(n)$, must be 0. In terms of the truth table for the first operation of MSD addition, as shown in Fig. 1(a), T_{n+1} must be 1. Furthermore, in terms of operation relation as shown in Fig. 4, the final addition result, S_{n+1} comes from the operations between T_{n+1} and T'_{n+1} . The operations are performed in accordance with third-operation rules of MSD addition, as shown in Fig. 3, in that no matter what value T'_{n+1} is, S_{n+1} is always 1 because $T_{n+1} = 1$. Therefore, each MSD addition as defined in Eq. (6) always makes the number of 1s reduced. In the same manner, for a negative Z_m , its most significant bit, $Z_m(n)$, must be $\bar{1}$, so the most significant bit of Z_m^- , $Z_m^-(n)$, must be $\bar{1}$ and the most significant bit of Z_m^+ , $Z_m^+(n)$, must be 0. In terms of the truth table for the third operation of MSD addition as shown in Fig. 3, no matter what value T'_{n+1} is, S_{n+1} is always $\bar{1}$ because $T_{n+1} = \bar{1}$. Therefore, each MSD addition as defined in Eq. (6) always makes the number of 1s reduced. In terms of the symmetry of 1 and $\bar{1}$ in the three operations of MSD addition, we can only consider the case for a positive Z_m .

In terms of the conversion method as defined in Eq. (6), we can conclude that no matter how many bits Z_m has, there are not the operations of 1 and 1, $\bar{1}$ and $\bar{1}$, and 1 and $\bar{1}$ during the addition between Z_m^+ and Z_m^- ; there are only the operations of 1 and 0, $\bar{1}$ and 0, and 0 and 0. Thus, the possibilities for T_{i+1} to be 1, 0, and $\bar{1}$ are all reduced to 2/3 of general cases in accordance with Fig. 1(a), and the possibilities for W_i to be 1 and $\bar{1}$ do not change, while the possibility to be 0 is reduced to 1/5 of general cases in accordance with Fig. 1(b). So, the possibilities for T'_{i+1} to be 1 and $\bar{1}$ are reduced to 2/3 of general cases; while according to Fig. 2(a), the possibility to be 0 is

$$\frac{\frac{2}{3} \times 2 + \frac{2}{3} \times \frac{1}{5} \times 2 + \frac{1}{5} \times 2 + \frac{1}{5} \times \frac{1}{3}}{7} = \frac{31}{105} < \frac{3}{10} \quad (7)$$

According to Fig. 2(b), the possibilities for W'_i to be 1 and $\bar{1}$ are

$$\frac{\frac{2}{3} \times \frac{1}{5} + \frac{1}{3}}{2} = \frac{7}{30} < \frac{3}{10} \quad (8)$$

and the possibility to be 0 is

$$\frac{\frac{2}{3} \times 4 + \frac{1}{5} \times \frac{1}{3}}{5} = \frac{41}{75} < \frac{6}{10} \quad (9)$$

Finally, according to Fig. 3, the possibility for S_i to be $\bar{1}$ is

$$\frac{\frac{2}{3} \times \frac{3}{10} + \frac{3}{10} \times \frac{3}{10} + \frac{6}{10} \times \frac{2}{3}}{3} = \frac{69}{300} < \frac{7}{30} < \frac{1}{4} \quad (10)$$

Therefore, each MSD addition makes the number of $\bar{1}$ in Z_m reduced to 1/4 of the original case at least.

With the assumption that an N -bit Z_m requires the conversions of n times, in terms of Eq. (10), we have

$$N' < \frac{N}{4^n} \quad (11)$$

where N' is the number of $\bar{1}$. Of course, if $N' < 1$ is required, only the following relation is required:

$$\frac{N}{4^n} \approx 1, \quad (12)$$

namely,

$$N \approx 4^n \quad \text{or} \quad n \approx \log_4 N. \quad (13)$$

In the binary addition, an N -bit addition generally requires the delay time that N carries, while each bit addition also requires about three logic operations such as AND, OR, and so on. Therefore, for the N -bit addition, the speed ratio between the MSD adder and binary ones is about

$$\beta \approx \frac{N}{n} \approx \frac{N}{\log_4 N}. \quad (14)$$

A plot of β versus N is shown in Fig. 19. It can be found from Fig. 19 that the more operand bits (i.e., data width), the higher the speed ratio between the MSD adder and binary ones, namely, the more obvious the advantage of the MSD system we presented herein. For a 32-bit Z_m , we perform the three times of conversion additions, then get a binary form as shown in Fig. 20, which agrees well with the approximate theoretical formula, Eq. (13). However, this parallel architecture of optoelectronic MSD adder and subtracter based on the SPLE scheme really has its own disadvantages. One important disadvantage is that it requires three times more hardware than the binary adder.

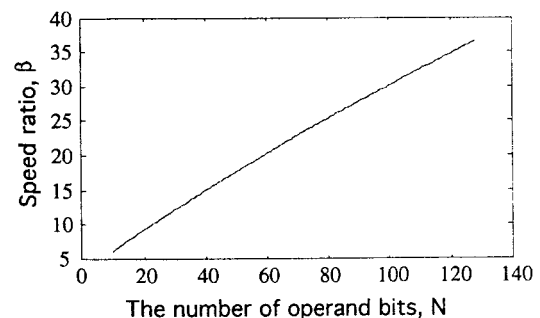


Fig. 19 Speed ratio relation curve of the MSD and binary additions with the number of operand bits N .

A 32-bit MSD number:

$$Z = 10\bar{1}\bar{1}\bar{1}\bar{1}0\bar{1}\bar{1}\bar{1}\bar{1}00\bar{1}\bar{1}\bar{1}0\bar{1}00\bar{1}\bar{1}\bar{1}\bar{1}\bar{1}\bar{1}0\bar{1}0\bar{1}0$$

After the first conversion addition:

$$Z_1 = 1\bar{1}0\bar{1}0\bar{1}00\bar{1}\bar{1}\bar{1}0\bar{1}00\bar{1}\bar{1}00\bar{1}\bar{1}00\bar{1}\bar{1}00\bar{1}00\bar{1}00\bar{1}0$$

After the second conversion addition:

$$Z_2 = 10\bar{1}0\bar{1}0\bar{1}00\bar{1}\bar{1}\bar{1}00\bar{1}\bar{1}0\bar{1}00\bar{1}\bar{1}00\bar{1}\bar{1}00\bar{1}00\bar{1}0$$

After the third conversion addition:

$$Z_3 = 10\bar{1}0\bar{1}\bar{1}00\bar{1}0\bar{1}\bar{1}00\bar{1}0\bar{1}00\bar{1}\bar{1}00\bar{1}\bar{1}00\bar{1}00\bar{1}0$$

Fig. 20 Thirty-two bit conversion example from MSD digits and binary ones.

7 Summary and Conclusions

In this paper, we discussed the characteristics of three stages of operations of MSD addition, and on this basis we proposed an SPLE scheme that not only makes best use of the convenience of binary logic operation but is also suitable for the trinary property of 1, 0, and $\bar{1}$ in MSD numbers. According to the truth tables of all the operations of MSD addition, we proposed a unitary optoelectronic switch module including nine detecting elements (G_1, \dots, G_9) to implement nine AND operations of any truth table, and on this basis we built the simplest butterfly architecture of an optically fully parallel MSD adder and subtracter. This butterfly network is two dimensional: one dimension is for implementing the interconnection among operand bits, which is completed electrically within switch modules now and will be completed optically in our next work, and other dimension is the simplest butterfly form for implementing the interconnection of two groups of operand digits in 1 bit, which is now completed optically. Finally, the 3-bit experimental model of a fully parallel MSD adder and subtracter was built using the simple optoelectronic switch technologies in conjunction with fiber interconnection technologies. At the same time, the simulation and the experimental results of MSD addition and subtraction are given.

In fact, not only can the 3-bit parallel MSD adder and subtracter be built using four optoelectronic switch modules and three stages of simple butterfly interconnects, as described in this paper, but any multibit parallel MSD adder and subtracter can also be built by using four switch modules and three stages of butterfly interconnects. Note that the simultaneous increases of operand data width and operation hardware, exactly like the analysis and comparison we did in Sec. 6, will take more time in the future research. The better trade-off between the operand data width and hardware is an important task to develop for the optoelectronic parallel MSD adder and subtracter discussed herein. After all, we have really implemented the effective combination of a parallel carry-free algorithm (MSD) and a parallel implementing architecture (optical multilayer butterfly interconnection), which is a new approach of high-speed digital optical computing. At the same time, we have also researched the optoelectronic multiplier²⁷ and divider and communication of this optoelectronic MSD computing system with binary electronic computers, which will be published in other papers. In our future work, we will use the micro-optoelectronic integration technology and micro-

structure interconnect technology to replace the current simple optoelectronic and fiber interconnect technologies to research and make the practical multibit optoelectronic parallel computing units.

Acknowledgments

This work was supported by both the Chinese Fundamental of Science and the Microelectronics Research Center of the University of Texas at Austin.

References

1. A. Avizienis, "Signed-digit number representations for fast parallel arithmetic," *IRE Trans. Electron. Comput.* **EC-10**, 389–398 (1961).
2. B. L. Drake, R. P. Bocker, M. E. Lasher, R. H. Patterson, and W. J. Miceli, "Photonic computing using the modified-digit number representation," *Opt. Eng.* **25**, 38–43 (1986).
3. K. Hwang and A. Louri, "Optical multiplication and division using modified-signed-digit symbolic substitution," *Opt. Eng.* **28**, 364–372 (1989).
4. Y. Li and G. Eichmann, "Conditional symbolic modified signed-digit content-addressable memory logic elements," *Appl. Opt.* **26**, 2328–2333 (1987).
5. A. K. Cherri and M. A. Karim, "Modified-signed digit arithmetic using an efficient symbolic substitution," *Appl. Opt.* **27**, 3824–3827 (1988).
6. J. U. Ahmed, A. A. S. Awwal, and M. A. Karim, "Two-bit trinary full adder design based on resisted signed digit numbers," *Opt. Laser Technol.* **26**, 225–229 (1994).
7. S. Zhou, S. Campbell, W. Wu, P. Yeh, and H. K. Liu, "Modified-signed-digit arithmetic for multi-input digital optical computing," *Appl. Opt.* **33**, 1507–1516 (1994).
8. D. Casasent and P. Woodford, "Symbolic substitution modified signed-digit optical adder," *Appl. Opt.* **33**, 1498–1506 (1994).
9. M. S. Alam, "Parallel optical computing using recoded trinary signed-digit numbers," *Appl. Opt.* **33**, 4392–4397 (1994).
10. A. K. Cherri, "Symmetrically recoded modified-digit optical addition and subtraction," *Appl. Opt.* **33**, 4378–4382 (1994).
11. H. Huang, M. Itoh, and T. Yatagan, "Modified signed-digit arithmetic based on redundant bit representation," *Appl. Opt.* **33**, 6146–6156 (1994).
12. B. Ha and Y. Li, "Parallel modified signed-digit arithmetic using an optoelectronic shared content-addressable-memory processor," *Appl. Opt.* **33**, 3647–3662 (1994).
13. M. A. Habli and K. Leonik, "Polarization-coded optical logic gates for N -inputs," *Optik* **91**, 100–102 (1992).
14. A. Louri, "Parallel implementation of optical symbolic substitution logic using shadow-casting and polarization," *Appl. Opt.* **30**, 540–548 (1991).
15. T. Yatagai, "Optical space-variant logic-gate array based on spatial encoding technique," *Opt. Lett.* **11**(4), 260–262 (1986).
16. K. Wong and L. M. Cheng, "Space-variant optical logic operations based on operation-dependent encoding method," *Appl. Opt.* **33**, 2134–2139 (1994).
17. J. Tanida, M. Iwata, and Y. Ichioka, "Extended coding for optical array logic," *Appl. Opt.* **33**, 3663–3669 (1994).
18. V. P. Heuring, L. H. Ji, R. J. Feuerstein, and V. N. Morozov, "Toward a free-space parallel optoelectronic computer: 300MHz optoelectronic interconnects," *Appl. Opt.* **33**, 7579–7587 (1994).
19. R. K. Kostuk, "Simulation of board-level free-space optical interconnects for electronic processing," *Appl. Opt.* **31**, 2438–2445 (1992).
20. D. G. Sun, N. X. Wang, L. M. He, M. Xu, G. D. Liang, and J. Zhang, "Research on optical multistage butterfly interconnection and optoelectronic logic operations," *Opt. Laser Technol.* **26**, 379–383 (1994).
21. P. Cinato and K. C. Young, Jr., "Optical interconnections within multipip modules," *Opt. Eng.* **32**, 852–860 (1993).
22. M. J. Murdocca, A. Huang, J. Jahns, and N. Streible, "Optical design of programmable logic arrays," *Appl. Opt.* **27**, 1651–1660 (1988).
23. J. Jahns and M. J. Murdocca, "Crossover networks and their optical implementation," *Appl. Opt.* **27**, 3155–3160 (1988).
24. F. B. McCormick and M. E. Prise, "Optical circuitry for free-space interconnections," *Appl. Opt.* **29**, 2013–2018 (1990).
25. D. G. Sun, Q. Xiang, N. X. Wang, and Z. H. Weng, "Butterfly interconnection implementation for an n -bit parallel adder/subtracter," *Opt. Eng.* **31**, 1568–1575 (1992).
26. K. M. Iftekharruddin and M. A. Karim, "Butterfly interconnection network: design of multiplier, flip-flop, and shift register," *Appl. Opt.* **33**, 1457–1462 (1994).
27. D. G. Sun, L. M. He, N. X. Wang, and Z. H. Weng, "Fast MSD multiplication technology and system," *Proc. SPIE* **2232**, 268–273 (1994).

De-Gui Sun received a BS degree from the Department of Fine Instrument and Optical Engineering, Harbin University of Technology, China, in 1985. He obtained an MS and PhD degrees from the Changchun Institute of Optics and Fine Mechanics, Chinese Academy of Sciences, in 1988 and 1993, respectively, where he was employed as an associate professor in 1993. Since 1994, he has been working as a postdoctoral fellow in the Microelectronics Research Center of the University of Texas at Austin. He has more than thirty publications in journals and international conference proceedings and a Chinese patent. He has earned the Third Grade of Natural Science Award '94 of Chinese Academy of Sciences, Jilin Young Scientist/Engineer Award '94 of China, and the President Scholarship '91 for Graduate Student of Chinese Academy of Sciences. His interests include optical and optoelectronic switching devices, optical and optoelectronic interconnects, digital optical and optoelectronic computing, and optical memory. Now he is a member of the Optical Computing Group of SPIE.

Na-Xin Wang received her BS degree from the Physical Department of Harbin Science and Technology University, China, in 1990. She obtained her MS degree from the Changchun Institute of Optics and Fine Mechanics, Chinese Academy of Sciences, in 1993. She has more than ten publications in journals and international conference proceedings and earned the President Scholarship '93 for Graduate Student of Chinese Academy of Sciences. Now she is a lecturer of the Wuxi Institute of Light Industrial Technology. Her interests include optical and optoelectronic switching devices, optical and optoelectronic interconnects, and digital optical and optoelectronic computing.

Liming He received a BS degree in electrical engineering at Dalian University of Technology, China, in 1985, and an MS degree in optics at the Changchun Institute of Optics and Fine Mechanics, Chinese Academy of Sciences, in 1989. She then was an assistant fellow, lecturer, and an associate professor of electronic engineering at the Jinlin University of Technology, China. She is currently a candidate for the PhD degree in precision engineering at the Chubu

University, Kasugai, Japan. Her interests include electronic circuits, optoelectronics, system control, and laser micromachining.

Zhao-Heng Weng received his BS degree from the physical department of the Yunnan University of China in 1958. Since then he has been working on laser science and its applications at the Changchun Institute of Optics and Fine Mechanics, Chinese Academy of Sciences, where was employed as a professor in 1986. His interests include nonlinear optics, adaptive optical processing, optical computing, and optical neural network.

Daheng Wang: Biography and photograph not available.

Ray T. Chen is currently a faculty member of the Microelectronics Research Center at the University of Texas, Austin. He was with Physical Optics Corporation, Torrance, California, from June 1988 to August 1992. He has been a principal investigator for more than forty awarded research proposals sponsored by many subdivisions of DOD, NSF, DOE, NASA and other private industries such as Cray Research, GE, Honeywell, Boeing, Physical Optics Corporation, and Novex Corp. His research topics cover 2-D and 3-D optical interconnections, polymer-based integrated optics, polymer waveguide amplifiers, graded index polymer waveguide lens, active optical backplane, traveling wave electro-optic polymer waveguide modulators, GaAs all-optical cross bar switch, holographic lithography, and holographic optical elements. He has served as the chairman and a program committee member for more than 20 domestic and international conferences organized by SPIE, IEEE, and PSC. He is also an invited lecturer for the short course of optical interconnects for the international technical meetings organized by SPIE. Dr. Chen has more than 150 publications including 25 invited papers. He has served as a consultant for various federal government agencies and private companies and delivered numerous invited talks in the professional societies. Dr. Chen is an active member of IEEE, LEOS, SPIE, OSA, and PSC.